Program Digest, 2019 IEEE International Ultrasonics Symposium (IUS)
Glasgow, Scotland, October 6-9, 2019

Differential frequency-domain photoacoustic microscope for blood oxygen saturation measurements

K. Sathiyamoorthy
Department of Physics
Ryerson University
iBEST, Keenan Research Centre
St.Michael's Hospital
Toronto, Canada, M5B 2K3

Michael C. Kolios
Department of Physics
Ryerson University
iBEST, Keenan Research Centre
St.Michael's Hospital
Toronto,Canada, M5B 2K3
mkolios@ryerson.ca

Abstract*—We have developed a low-cost frequency domain differential photoacoustic microscope. The microscope uses a low-cost PA sensor made up of a kHz microphone, low power CW lasers and an optical chopper with 6/5 dual-slot disc. The system used dual-slot chopper disc to modulate two laser beams simultaneously and the corresponding PA signals were measured. This simultaneous modulation enabled a single scan instead of two scans required for two lasers in previous configurations, reducing the scanning time half. The configuration also enabled two PA interrogations at the same location of the sample whereas in the conventional sequential measuring system any backslash of the translation stage would alter the location of the interrogation area during the next measurement. The developed sensor is used to study the oxygen saturation of a single RBC. Two types of RBCs containing predominately oxy and methemoglobin were investigated using three different lasers of wavelengths 473 nm, 533 nm, and 633 nm. The single cell study showed that half of the oxy-RBC and meth-RBC exhibit oxygen saturation of about 90 % and 38.61 % respectively.

Keywords*—differential, frequency domain, red blood cell, methemoglobin, oxygen saturation, histogram

I. Introduction

Blood oxygen saturation studies involve the measurement of hemoglobin in the blood that carries oxygen. A false reading might occur if the method fails to identify hemoglobin binding to other species such as carbon monoxide. Pulse oximetry is the most commonly used method to study the oxygen saturation.[1]–[3] However, this technique fails to give the correct estimate in people experiencing hypoxia due to carbon monoxide poisoning and methemoglobinemia since it exclusively depends on the measurement of oxygen bounded hemoglobins. Multispectral photoacoustic could provide a solution as it provides functional information, but hardware cost hinders clinical adaptation.[4]–[8] We have developed a low-cost differential frequency-domain photoacoustic microscope to overcome these shortcomings.[9] The system uses a low-cost PA sensor and CW lasers. The PA sensor was developed using a kHz microphone. The sensor was designed in a unique configuration to amplify the weakly generated PA signal by a low power CW laser. The main feature of this configuration is a resonator used to amplify the weak signal generated by a low power laser. The strength of the PA signal is proportional to the thermal diffusion length in the sample, which is a function of laser amplitude modulation frequency. The thermal diffusion length in the sample is given by [10]

$$\mu = \frac{k}{\pi \rho f c} \tag{1}$$

where k is the thermal conductivity, ρ the density, c the specific heat and f is the modulation frequency.

One advantage of the sensor is it works in a non-contact mode. There is no coupling medium required as in the case of conventional PA detection, which denatures and alter the sample original properties in some cases. Both dry and liquid sample can be used for the measurement in the present system. The sensor can be used in both epi and trans-illumination microscope as the microphone in the sensor never obstructs the interrogated light from the microscope and/or any other optical paths as it lies away from the sample due to the presence of the resonator. This configuration would enable the straight forward integration of other probing systems such as optical, fluorescent, Raman, SERS and PA imaging for multimodal imaging. In this article, we discuss the development of the system and its application in blood oxygen studies.

II. Materials and Methods

A. Procurement of Blood

Human blood was collected by netCAD (Vancouver, Canada), the research division of Canadian Blood Services, under protocol 2013-001, which involves standard Canadian Blood Services collection and testing procedures of whole blood and delivery overnight at 4°C, with continuous monitoring during shipment to ensure no temperature deviations occur. This procedure has been approved by the research ethics boards.

B. Blood sample preparation

The guidelines on handling the blood were followed in accordance with the recommendations of the International Society for Clinical Hemorheology and the European Society for Clinical Hemorheology and Microcirculation.[11] The blood was centrifuged at room temperature at 2000 × g for 6 min to separate the plasma and their Buffy coat. Isotonic phosphate-buffered saline (PBS) was used to wash RBCs two times. The centrifuged RBCs were then dispersed in PBS. Two types of RBCs, oxy and methemoglobin, were studied. Methemoglobin was prepared by treating RBC with sodium nitrate (NANO3). Two mg of NANO3 were mixed with 1 ml of blood and shaken well. The optical absorption properties of the samples were studied using a USB 4000 Ocean optics fiber optics spectrometer. The glass slide was ultrasonically cleaned using isopropyl alcohol followed by water to remove any trace of oil or dirt. Both treated (meth) and untreated RBCs (oxy) were smeared on microscope slides for studies.

C. Experimental setup

The PA system uses low power continuous-wave lasers (473 nm, 533 nm, and 633 nm) of power 3-4 mW and a photoacoustic resonant sensor that incorporates a kHz microphone. The system measures two PA signals by employing two lasers simultaneously modulated at two different modulation frequencies (finner = 238 and fouter = 285 Hz) and instantaneously un-mixes these using the lsqlin function in MATLAB (Mathworks Inc.). This approach reduces the scanning time by half since other systems require separate measurements for each wavelength. The output of the laser was mechanically modulated using SR540 optical chopper. Two different modulation frequencies were achieved by using 6/5 dual-slot chopper blade. This 6/5 dual-slot chopper blade contains five openings for light in the inner row (I) and six openings in the outer row (O). The lasers beams which are passed through these dual slots will be modulated at two different frequencies. The modulated beams then combined into a single beam by a mirror (M1). The PA signals corresponding to two modulation frequencies were measured using SR850 and SR510 lock-in amplifiers. The measured PA signals were unmixed using the lsqlin function in MATLAB.

The PA system is integrated with the custom-made optical microscope system to visualize the sample. The optical system is built in an inverted configuration. The system is made of an infinity-corrected 40X and 0.25 NA Olympus objective (O), a Ximea xiQ camera (Ximea, USA) and white LED (Thorlabs, USA). The sample is imaged from the bottom with the illumination source (LED) on the top. The position of the sample can be changed/raster scanned using the X-Y linear stage (Thorlabs, USA).

The sample for PA studies is taken in a sample chamber of a PA sensor. The PA sensor contains a sample chamber to hold the sample and a microphone (type 4189, Brüel & Kjær Sound & Vibration Measurement, Pointe-Claire, Quebec, Canada) to measure the PA signal. The sample chamber and the microphone are connected by the resonator. The resonator helps to amplify the PA signal and protect the microphone from the scattered light form the sample. The size of the sample chamber and the length of the resonator are 8mm x 3mm and 100 mm respectively. The sensor is made of acrylic polymer. The details of the sensor can be found in previous publications.[10]

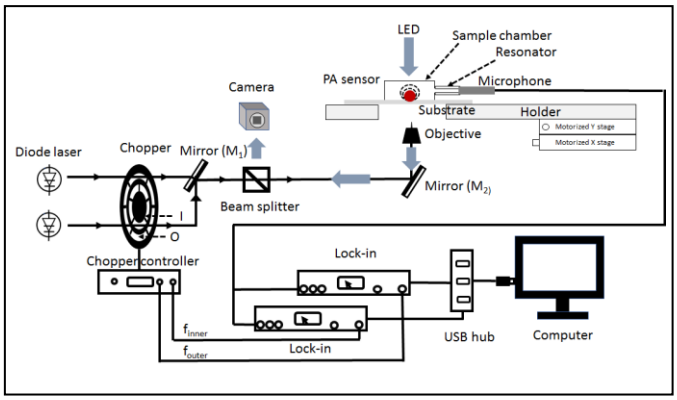

Fig. 1. Schematic diagram of the differential frequency-domain photoacoustic microscope.

The application of the proposed differential technique was investigated on two types of red blood cells (RBCs) containing predominantly oxy and methemoglobin. Methemoglobin was prepared by treating RBCs with sodium nitrate (NANO3) for a few seconds. Both treated and untreated samples were smeared on a glass substrate for studies. About 5 – 10 RBCs were characterized in each group.

III. Results and Discussion

Whole blood exhibits optical absorption peaks in the visible region at 420 nm, 540 nm, and 578 nm. These peaks 540 nm and 578 nm are called Q band peaks due to singlet state transition from S0 to S1. The transitions are due to electron transfer from π to π* porphyrin ring orbitals within the porphyrin ligand.[12], [13] This can be explained by Gouterman Four-Orbital Model.[12] According to this model, the optical absorption in porphyrins is due to the electronic transition between two HOMOs and two LUMOs orbitals. Any structural change would split these two states of energy into a higher energy state with greater oscillator strength, giving rise to the Soret band, and a lower energy state with less oscillator strength giving rise to the Q-bands. The optical absorption increase below 470 nm is due to the strong Soret band transition.

A healthy human possesses methemoglobin in concentrations < 1% of total hemoglobin that is formed by spontaneous slow auto-oxidation of hemoglobin. Methemoglobin subsequently reduced to hemoglobin to maintain a steady-state of methemoglobin concentration in whole blood. People suffer from methemoglobinemia possess an abnormal amount of methemoglobin. Methemoglobinemia can be either inherited or acquired. The inherited methemoglobinemia is genetically transferred whereas acquired methemoglobinemia is produced by the action of oxidants. When an individual is exposed to an exogenous oxidizing agent, the rate of methemoglobin formation can

overwhelm the protective reduction mechanisms resulting in a condition called acquired methemoglobinemia.[14]

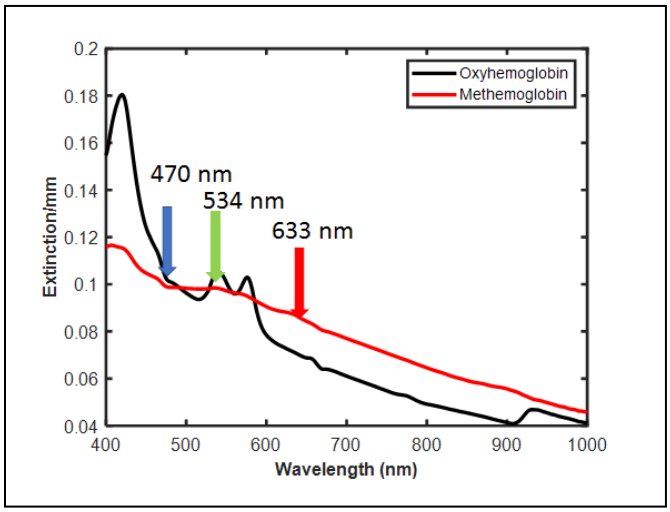

Fig. 2. Measured optical extinction spectra of Oxyhemoglobin and methemoglobin.

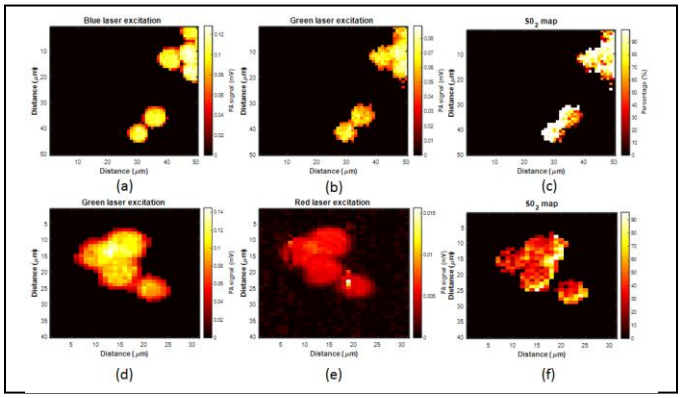

Fig. 3. PA image of oxy-RBCs using blue and green laser excitation (c) sO2 map obtained using the constrained linear least-squares solver on figures (a and b), (d) and (e) PA image of treated RBCs (Methemoglobin) and (f) sO2 map of the sample (d and e).

The solid red line in absorption spectrum of Figure 2 represents a RBC containing methemoglobin. In these experiments, methemoglobin is obtained by oxidizing hemoglobin using NaNO3 which can be reduced back to hemoglobin using methylene blue.[15] The iron Fe2+ (ferrous) in the heme group is oxidized to Fe3+ (ferric) state. This conformational change would inhibit bonding new free oxygen. This change inhibits the unloading of the bonded oxygen in tissues and predisposes the tissues to hypoxia due to an increased affinity towards its own bounded oxygen. This change would be observed as a leftward shift of the oxygen dissociation curve. The optical absorption spectrum of methemoglobin showed a small peak at 406 nm and 534 nm are left-shifted with respect to the peaks of oxyhemoglobin. There is a broad absorption shoulder around 630 nm further confirms the formation of methemoglobin.

Figure 3 shows PA images of treated (meth) and untreated RBCs (oxy). Figure 3 (a) and (b) are the PA image of untreated RBCs due to excitation by 473 nm and 533 nm lasers. Figure 3 (d) and (e) are the PA image of treated RBCs due to excitation at 533 nm and 633 nm wavelength lasers. A linear least-squares algorithm was used to calculate the percent sO2 value at each pixel. The resultant sO2 maps of RBC smears are shown in the last column of figure 3.

The histogram analyses of sO2 distribution showed that oxy-RBC exhibited mean, median and mode SO2 values of 79%, 90%, and 100% respectively. The RBCs treated with sodium nitrate exhibited mean, median, and mode SO2 values of 42.46%, 38.61%, and 24.32% respectively. The median SO2 value of oxy-RBC indicates that 50 % of the cells exhibit about 90% oxygen saturation whereas the treated RBC exhibit a low oxygen saturation of about 38.61 %. The peak mode of histogram of oxy-RBC suggested that chromophores of oxygen saturation around 100% were most commonly distributed in the cell. However, in the case of the treated cells, chromophores of oxygen saturation around 24.32% were commonly present. The system developed can be used to study the functional parameters of cellular chromophores

IV. Conclusion

A low-cost frequency domain differential photoacoustic microscope was developed to study the optical and acoustic properties of the biological samples. The system saves the measurement time by doing two PA measurements simultaneously and enables the laser excitations at the same location of the sample, which avoids a backslash-associated error due to the translation stage and position errors due to sample vibration. The potential application of this system was demonstrated on a single RBC by studying its oxygen saturation at a micron resolution. The developed system can be used to monitor blood oxygen saturation and bilirubin concentration in real time. Traditionally a CO-oximeter, pulse oximeter and blood gas analyzer are used to study methemoglobin. A subcutaneous bilirubinometer has been used for bilirubin studies. The developed PA imaging approach can be used to study these properties, and further enable the study of opaque samples such as highly concentrated methemoglobin.

Acknowledgment

This work was funded by the Natural Sciences and Engineering Research Council of Canada (RGPIN-2017-06496) and Ryerson University. Funding to purchase the equipment was provided by the Canada Foundation for Innovation, the Ontario Ministry of Research and Innovation, and Ryerson University.

References

[1] A. Jubran, “Pulse oximetry,” Crit. Care, vol. 19, no. 1, p. 272, Jul. 2015.

[2] M. Nitzan, A. Romem, and R. Koppel, “Pulse oximetry: fundamentals and technology update,” Med. Devices Auckl. NZ, vol. 7, pp. 231–239, Jul. 2014.

[3] C. D. Hanning and J. M. Alexander-Williams, “Pulse oximetry: a practical review,” BMJ, vol. 311, no. 7001, pp. 367–370, Aug. 1995.

[4] T.-H. Bok, E. Hysi, and M. C. Kolios, “Simultaneous assessment of red blood cell aggregation and oxygen saturation under pulsatile flow using high-frequency photoacoustics,” Biomed. Opt. Express, vol. 7, no. 7, pp. 2769–2780, Jun. 2016.

[5] E. Hysi, L. A. Wirtzfeld, J. P. May, E. Undzys, S.-D. Li, and M. C. Kolios, “Photoacoustic signal characterization of cancer treatment response: Correlation with changes in tumor oxygenation,” Photoacoustics, vol. 5, pp. 25–35, Mar. 2017.

[6] M. Li, Y. Tang, and J. Yao, “Photoacoustic tomography of blood oxygenation: A mini review,” Photoacoustics, vol. 10, pp. 65–73, May 2018.

[7] L. V. Wang and S. Hu, “Photoacoustic Tomography: In Vivo Imaging from Organelles to Organs,” Science, vol. 335, no. 6075, p. 1458, Mar. 2012.

[8] K. Sathiyamoorthy, Eric M. Strohm, and Michael C. Kolios, “Multispectral photoacoustic bioimaging using low power continuous wave lasers,” presented at the Proc.SPIE, 2017, vol. 10064.

[9] Krishnan Sathiyamoorthy, Eric M. Strohm, and Michael C. Kolios, “Low-power noncontact photoacoustic microscope for bioimaging applications,” J. Biomed. Opt., vol. 22, no. 4, pp. 1–7, Apr. 2017.

[10] S. Krishnan and M. C. Kolios, “Experimental design and numerical investigation of a photoacoustic sensor for a low power continuous wave laser-based frequency-domain photoacoustic microscopy,” J. Biomed. Opt., (Under review).

[11] O. K. Baskurt et al., “New guidelines for hemorheological laboratory techniques,” Clin. Hemorheol. Microcirc., vol. 42, no. 2, pp. 75–97, 2009.

[12] M. L.R., The Colours of Life: An Introduction to the Chemistry of Porphyrins and Related Compounds, 1st ed. Oxford University Press, 1997.

[13] Porphyrins, Ed. D. Dolphin. New York: Academic Press, 1978.

[14] L. L. Gutenberg, J.-W. Chen, and L. Trapp, “Methemoglobin Levels in Generally Anesthetized Pediatric Dental Patients Receiving Prilocaine Versus Lidocaine,” Anesth. Prog., vol. 60, no. 3, pp. 99–108, 2013.

[15] L. Gharahbaghian, B. Massoudian, and G. DiMassa, “Methemoglobinemia and Sulfhemoglobinemia in Two Pediatric Patients after Ingestion of Hydroxylamine Sulfate,” West. J. Emerg. Med., vol. 10, no. 3, pp. 197–201, Aug. 2009.